ACS APPLIED MATERIALS & INTERFACES

www.acsami.org

Research Article

Enhanced Photovoltaic Effect in *n*-3C-SiC/*p*-Si Heterostructure Using a Temperature Gradient for Microsensors

Hung Nguyen,* Thanh Nguyen, Duy Van Nguyen, Hoang-Phuong Phan, Tuan Khoa Nguyen, Dzung Viet Dao, Nam-Trung Nguyen, John Bell, and Toan Dinh*

Cite This: *ACS Appl. Mater. Interfaces* 2023, 15, 38930−38937

Read Online

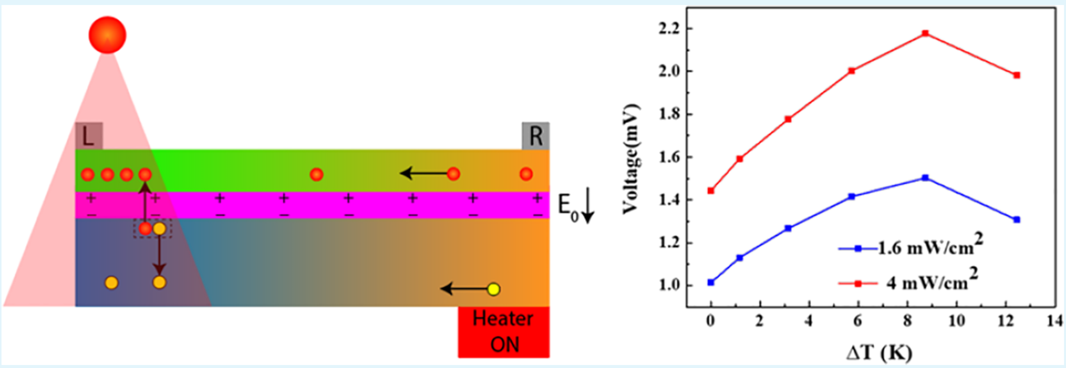

ABSTRACT: The development of fifth-generation (5G) communications and the Internet of Things (IoT) has created a need for high-performance sensing networks and sensors. Improving the sensitivity and reducing the energy consumption of these sensors can improve the performance of the sensing network and conserve energy. This paper reports a large enhancement of the photovoltaic effect in a 3C-SiC/Si heterostructure and the tunability of the photovoltage under the impact of a temperature gradient, which has the potential to increase the sensitivity and reduce the energy consumption of microsensors. To start with, cubic silicon carbide (3C-SiC) was grown on a silicon wafer, and a micro-3C-SiC/Si heterostructure device was then fabricated using standard photolithography. The result revealed that the sensor could either capture light energy, transform it into electrical energy for self-power purposes, or detect light with intensities of 1.6 and 4 mW/cm^2. Under the impact of the temperature gradient induced by conduction heat transfer from a heater, the measured photovoltage was improved. This thermo-phototronic coupling enhanced the photovoltage up to 51% at a temperature gradient of 8.73 K and light intensity of 4 mW/cm^2. Additionally, the enhancement can be tuned by controlling the direction of the temperature gradient and the temperature difference. These findings indicate the promise of the temperature gradient in SiC/Si heterostructures for developing high-performance temperature sensors and self-powered photodetectors.

KEYWORDS: *thermo-phototronic, photodetector, temperature sensor, microsensors, temperature gradient, silicon carbide heterostructure*

■ INTRODUCTION

As the world moves toward the implementation of 5G wireless networks and the integration of IoT,[1,2] technical devices available for these technologies have seen a significant expansion.[3] This shift has led to a marked increase in both the quantity of sensing devices and their energy sources.[4] Currently, batteries are the most utilized method for powering these devices; however, this approach comes with several disadvantages such as potential environmental pollution, limited life span, and costly maintenance,[5−8] and as an alternative, self-powered sensors that are able to capture energy from the environment and do not rely on batteries may be a more appropriate solution to address these challenges.[9−11] Light and thermal energy are the most readily available forms of energy in the environment[12,13] and often can be found together. For instance, both light and thermal energy can be emitted simultaneously from sources such as the sun, light bulbs, computer monitors, and even fires. Therefore, developing sensors that can capture both light and thermal energy simultaneously and use them to power themselves is an ideal solution to take advantage of these abundant energy sources.[14,15]

Received: May 10, 2023
Accepted: July 24, 2023
Published: August 2, 2023

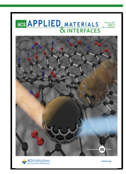

https://doi.org/10.1021/acsami.3c06699
ACS Appl. Mater. Interfaces 2023, 15, 38930−38937

There are some previous reports on self-powered sensors that can utilize light energy and thermal energy.[16−18] However, new sensing technology development is still needed to attain sensors that are more efficient, more readily available, and more compact in size.[19−21] Thus, a compact self-powered sensor that can capture light energy and function well in hot environments would be the perfect answer to the mentioned issues.[22] For self-powered sensing applications, SiC/Si heterostructure-based photodetectors have recently gained a lot of attention.[23,24] There are some reports showing that using the temperature gradient can substantially improve the photovoltage of semiconductors,[1,25−29] known as the thermo-phototronic effect. However, there have been very limited reports on the effect of the temperature gradient on the photovoltaic effect of the SiC/Si heterostructure. Recent studies have shown the huge potential of the SiC/Si heterostructure for numerous sensing applications and devices such as photodetector,[23] strain sensor,[12] temperature sensor,[30] position detector,[31] and gas sensor.[32] Due to the robustness of the SiC coating layer, the SiC/Si heterostructure-based sensors can work effectively in severe conditions.[33,34] Therefore, a comprehensive understanding of the sensing mechanism that governs the thermo-phototronic effect in the SiC/Si heterostructure will push forward its big potential as a microsensor for high-performance sensing systems as well as niche applications such as high operating temperatures.

In this study, we apply a new method of using a temperature gradient to enhance the performance of photodetectors up to 51% using a *n*-SiC/*p*-Si heterostructure. Our study for the first time presents an effective strategy to enhance the photovoltage using the thermo-phototronic effect in the lateral direction of a heterojunction device. We discover specific conditions for the heterostructure that can couple the lateral temperature gradient with the photoexcitation of charge carriers at the heterojunction device to enhance the sensitivity. We also study the sensing mechanism in the SiC/Si heterostructure to understand the unusual response of the device under a lateral temperature gradient. We first describe the fabrication of a microsensor from a monolithic design structure of *n*-type 3C-SiC grown on *p*-type Si that can sense light and use it as a power supply. The sensor has zero power consumption due to the generation of the photovoltage under the light intensities of 1.6 and 4 mW/cm^2. To evaluate the sensor's ability to convert energy, we study photovoltage generation under the illumination of controlled light from a red-light laser beam. The energy level of the red light (frequency of 635 nm) is approximately 1.95 eV, which exceeds the band gap of Si (1.12 eV) but falls short of the band gap of 3C-SiC (2.3 eV).[35,36] Therefore, red light can effectively penetrate the thin SiC layer and generate electron−hole pairs (EHPs) in the Si layer upon absorption. Besides, the microsensor also has the capability to capture heat and use the temperature gradient to increase its sensitivity. Additionally, we comprehensively evaluate the thermo-phototronic effect in the 3C-SiC/Si heterostructure using a red laser and a heater which generates a temperature gradient by thermal conduction. Under the conditions of just illumination and without any ambient temperature, the sensors can capture light and convert it to electrical energy with photovoltages of 1.01 and 1.44 mV under 1.6 and 4 mW/cm^2 laser beams, respectively. Under both illumination and heat conditions, the voltage reached a maximum of 2.18 mV under a temperature gradient of 8.73 K. The subsequent enhancement ratio of photovoltage was 51% as a result of the coupling between the temperature gradient and lateral illumination.

RESULTS AND DISCUSSION

A 100 nm thick *n*-type 3C-SiC layer was developed on a *p*-type Si wafer using a low-pressure chemical vapor deposition process, as described in the Experimental Section. Figure 1a

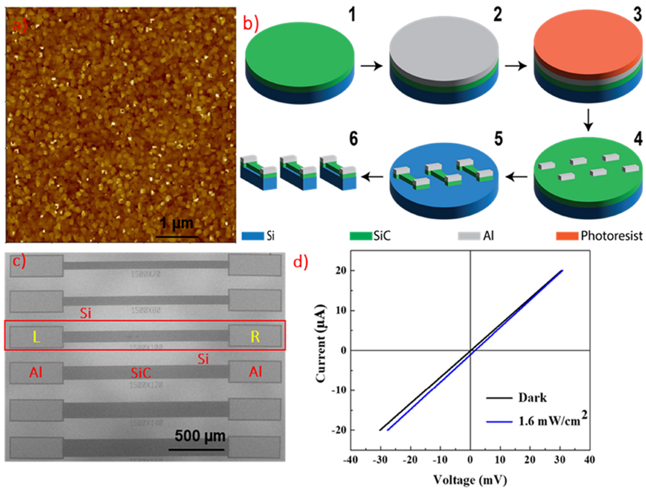

Figure 1. (a) AFM image of a 5 μm × 5 μm region of the 3C-SiC film. (b) Fabrication process. (c) SEM image of the device. (d) $I-V$ characteristics of the device at dark condition and 1.6 mW/cm^2 illumination.

shows the AFM image of the as-grown SiC layer. The AFM picture of a 5 μm × 5 μm region indicates a surface roughness of 1.48 nm for the SiC layer, which suggests that the SiC layer has been grown evenly. Figure 1b shows the process flow for the fabrication of a SiC/Si heterostructure device utilizing the standard photolithography and etching processes. Figure 1c shows the SEM image of the fabricated sensors. The sensor was designed with an I-shaped layer of SiC and two rectangular Al electrodes. The dimensions of the SiC bridge are 1500 μm in length and 100 μm in width. To measure the lateral photovoltaic effect, we have connected the electrodes solely on the *n*-3C-SiC layer; each electrode has dimensions of 450 μm in length and 200 μm in width. The gap between the electrodes is sufficient to create a temperature gradient of up to 8.73 K. For practical applications, it is important to carefully consider the dimensions of the devices for optimizing the thermal distribution and maximizing the efficiency of photovoltaic generation. The compact design allows the microsensor to be easily integrated into various applications, and the small form factor enables it to be easily transported, making it convenient to use in different environments. Figure 1d shows the typical current−voltage ($I-V$) properties of the 3C-SiC/Si structure under dark conditions and at a light intensity of 1.6 mW/cm^2, which confirmed the Ohmic contact. The linear pattern of the $I-V$ characteristics shows that there is an Ohmic contact between aluminum electrodes and the SiC/Si heterostructure-based device at the tested conditions.

Figure 2a shows the measured photovoltage response of the SiC/Si heterostructure under illumination from a red laser beam with intensities of 1.6 and 4 mW/cm^2. The experiment was conducted by illuminating the electrodes with a laser beam of different intensities and applying different temperature gradients. Without light and temperature gradient, the voltage

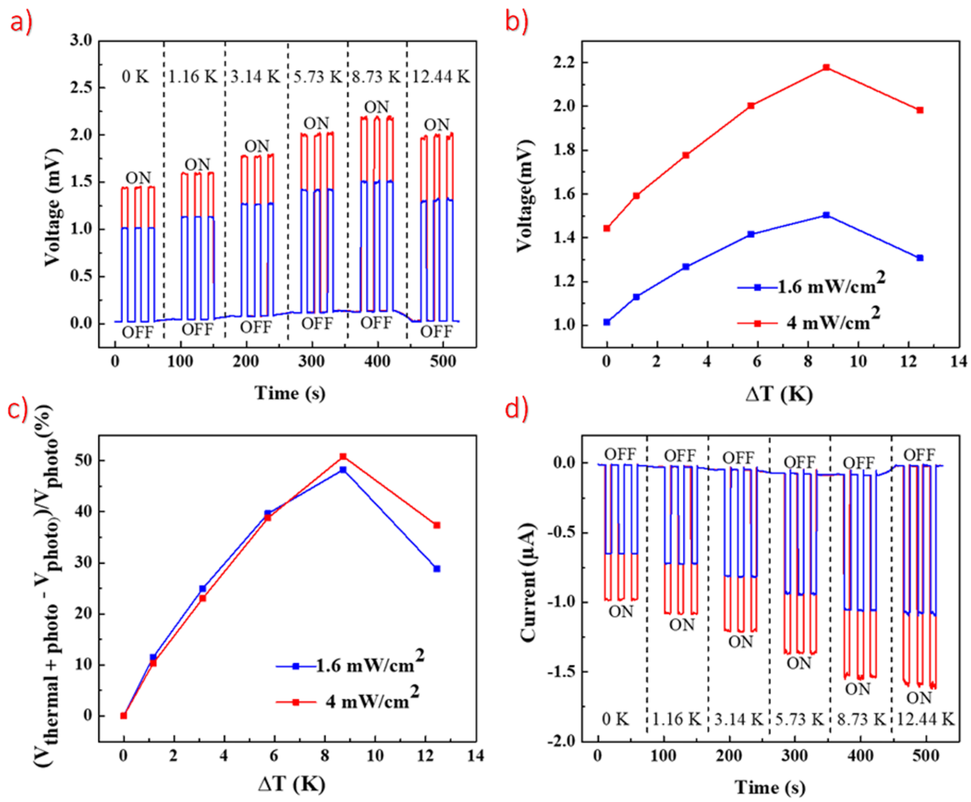

Figure 2. Sensitivity enhancement of a photodetector by a lateral thermal gradient: illuminating the electrode L and heating the electrode R. (a) Real-time-generated voltage under illumination and temperature gradient. (b) Dependence of an open-circuit voltage by ΔT. (c) Improvement of voltage by ΔT. (d) Real-time-generated current. The red lines represent 4 mW/cm^2, and the blue lines represent 1.6 mW/cm^2.

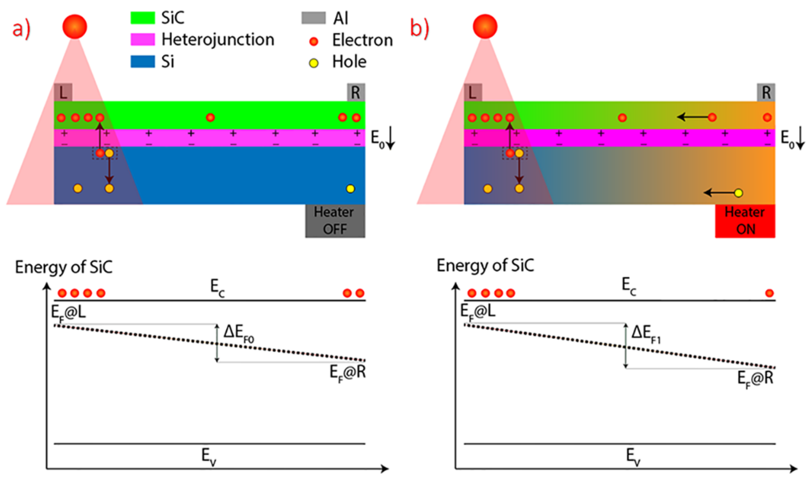

Figure 3. Mechanism of sensitivity enhancement of the photodetector by a lateral thermal gradient. (a) Illuminating the electrode L: creation of EHPs when a material is excited by photons, the formation of an uneven distribution of electrons in a 3C-SiC layer, and the band structure of 3C-SiC under nonuniform light. (b) Illuminating the electrode L and heating the electrode R: creation of EHPs through both photonic and thermal stimulation, the distribution of electrons in 3C-SiC, and the band structure of 3C-SiC.

was nearly zero, and upon exposure to light with the intensities of 1.6 and 4 mW/cm^2, it quickly rose to approximately 1.01 and 1.44 mV, respectively. By turning the laser source on and off three times, with 10 s interval between each cycle, the lateral photovoltage generated displayed excellent repeatability, as demonstrated in Figure 2a. This repeatability suggests that the effect is reproducible and consistent, making it a reliable source of energy generation.

The process of converting light energy to electrical power is facilitated by the photovoltaic effect in the 3C-SiC layer. Figure 3a illustrates the conversion mechanism from the photon energy from a laser beam to electrical power, as demonstrated by the voltage generated between the electrodes L and R. The laser beam is focused on the electrode L of the sensor. Upon illumination, numerous photons are introduced and captured in the heterojunction area and Si layer near the heterojunction. Due to its relatively thin thickness and wide energy band gap, the 3C-SiC layer is permeable to the red wavelength. Owing to its high energy of approximately 1.95 eV, the red laser can generate free electrons and free holes in the Si layer, resulting

https://doi.org/10.1021/acsami.3c06699
ACS Appl. Mater. Interfaces 2023, 15, 38930−38937

in the formation of EHPs in the Si layer. Within the heterojunction area, the movement of charge carriers is influenced by the internal electric field. In a n-3C-SiC/p-Si heterostructure, the electric field is oriented from the 3C-SiC layer toward the Si substrate (Figure 3a). As a result, electrons are directed into the n-3C-SiC layer when holes are directed into the p-Si layer, resulting in a higher electron concentration in the illuminated area compared to the dark area. The Fermi levels in n-3C-SiC at the electrode L and electrode R can be given by:[37]

$$E_{F@L} = E_C - k_B \cdot T \cdot \ln \frac{N_{C@L}}{N_{D@L}} \tag{1}$$

$$E_{F@R} = E_C - k_B \cdot T \cdot \ln \frac{N_{C@R}}{N_{D@R}} \tag{2}$$

where E_C is the conduction band energy of 3C-SiC, k_B is the Boltzmann constant, T is the absolute temperature, $N_{C@L}$ and $N_{C@L}$ are the effective density of states in the conduction band at the electrode L and R, respectively, and $N_{D@L}$ and $N_{D@R}$ are the electron concentrations at the electrodes L and R, respectively.

Since $N_{D@L}$ is higher than $N_{D@R}$, $E_{F@L}$ is higher than $E_{F@R}$, and the Fermi level in the n-SiC layer is bent from the electrode R to electrode L.

When only illuminating the device, the temperature gradient across it was not observed. Therefore, any impact of the pyroelectric effect remains unclear in this study. However, we observed an improvement in photovoltage when the external heater was turned on. Figure 2b shows the dependence of photovoltage on the temperature gradient. As the temperature gradient increased from 0 to 8.73 K, the photovoltage increased gradually. The highest photovoltage values peaked at around 1.5 and 2.18 mV for light intensities of 1.6 and 4 mW/cm^2, respectively. It is worth mentioning that the results obtained by repeatedly switching on and off the laser power source within the context of the varying temperature gradients were consistently reliable. When the temperature difference between the two electrodes increased to 12.44 K, with the left electrode at 439.66 K and the right electrode at 427.22 K, the photovoltage decreased to approximately 1.31 and 1.98 mV, respectively.

Figure 2c illustrates the enhancement of photovoltage when the device was exposed to varying temperature gradients, as compared to a baseline condition without a temperature gradient. Under an illumination intensity of 1.6 mW/cm^2, an increase in temperature gradient from 0 to 1.16, 8.73, and 12.44 K resulted in a corresponding increase in the generated photovoltage of approximately 11, 48, and 29%, respectively. When the device was illuminated at an intensity of 4 mW/cm^2, the data also revealed an increase in the photovoltage of 10, 51, and 37% at the previously mentioned temperature gradients 1.16, 8.73, and 12.44 K, respectively. The photovoltage enhancement of up to 51% indicates the potential of using the SiC/Si heterostructure for an ultrasensitive photodetector. The 51% increase in voltage using a temperature gradient for n-SiC/p-Si is comparable to the 21.9% reported for P3HT/ZnO, 31.8% reported for Na-doped SnS, 75% reported for BiFeO3, and 76% reported for the InP/ZnO heterostructure, as shown in Table S1.[25,29,38,39]

When a lateral temperature gradient is applied to the 3C-SiC/Si heterostructure by activating the heater beneath the electrode R, the thermal gradient can induce the diffusion of both electrons and holes within the SiC semiconductor. Figure 3b illustrates the production of EHPs using photonic and thermal stimulation, the band structure of 3C-SiC, and the distribution of electrons in 3C-SiC. As the majority carriers in n-SiC are electrons and the minority carriers are holes, the electrons will exhibit a tendency to migrate from the hotter region to the cooler region, while the holes will tend to shift in the opposite direction. The application of the temperature gradient causes the Fermi level at the electrode L to be elevated due to the increased diffusion of electrons toward it, while the Fermi level at the electrode R is lowered as a result of the diffusion of electrons away from the hot region (Figure 3b). The simultaneous application of heating the region under the electrode R and illuminating the top of the electrode L results in an exceptional electron concentration gradient across the n-SiC layer, yielding a higher voltage output compared to either heating or illuminating alone.

The voltage difference between two electrodes (which have the temperature gradient between them) is described as follows:

$$\Delta V = S \times \Delta T \tag{3}$$

where S is the Seebeck coefficient of the n-SiC layer, and ΔT is the temperature difference between the two electrodes.[37]

Consequently, the progressive increase in the temperature gradient from 1.16 to 8.73 K led to a corresponding rise in the voltage difference between the electrode L and electrode R. When the temperature gradient reached 12.44 K in this study, the voltage between the electrodes started to decrease. This is due to the experimental setup where only electrode R was heated, and electrode L was cooled by the surrounding room temperature. To reach a temperature gradient of 12.44 K, electrode R was heated to approximately 440 K, which increases the probability of exciting electrons to the conduction band from the valence band of Si, resulting in a substantial production of electrons around electrode R thanks to the built-in potential E_o at the heterojunction. The quantity of electrons produced from heating electrode R to 440 K exceeded the number of electrons that were pushed toward electrode L by the temperature gradient. When the temperature is high enough to promote the electrons to the conduction band of Si, the Si layer becomes more conductive, and this reduces the charge gradient between the two electrodes, lowering the recorded photovoltage. As a result, the accumulated electrons around the electrode R weakened the electron gradient between the two electrodes created by illuminating electrode L. More details of the temperatures at each electrode and the temperature difference between them can be found in Table S2.

Figure 2d presents a real-time response of the photocurrent under varying illuminating conditions and temperature gradients. When the device was in darkness and without any temperature gradient, the photocurrent generated was negligible. However, when illuminated with light intensities of 1.6 and 4 mW/cm^2, the recorded currents were −0.65 and − 1 μA, respectively. Furthermore, when the light intensity was held constant at 1.6 mW/cm^2 and the temperature gradient rose from 0 to 12.44 K, the photocurrent decreased gradually from nearly 0 to −1.09 μA. Additionally, when the light intensity was held at 4 mW/cm^2 and the temperature gradient was increased to 12.44 K, the measured current gradually decreased to −1.6 μA. This illustrates that as the light intensity

https://doi.org/10.1021/acsami.3c06699
ACS Appl. Mater. Interfaces 2023, 15, 38930−38937

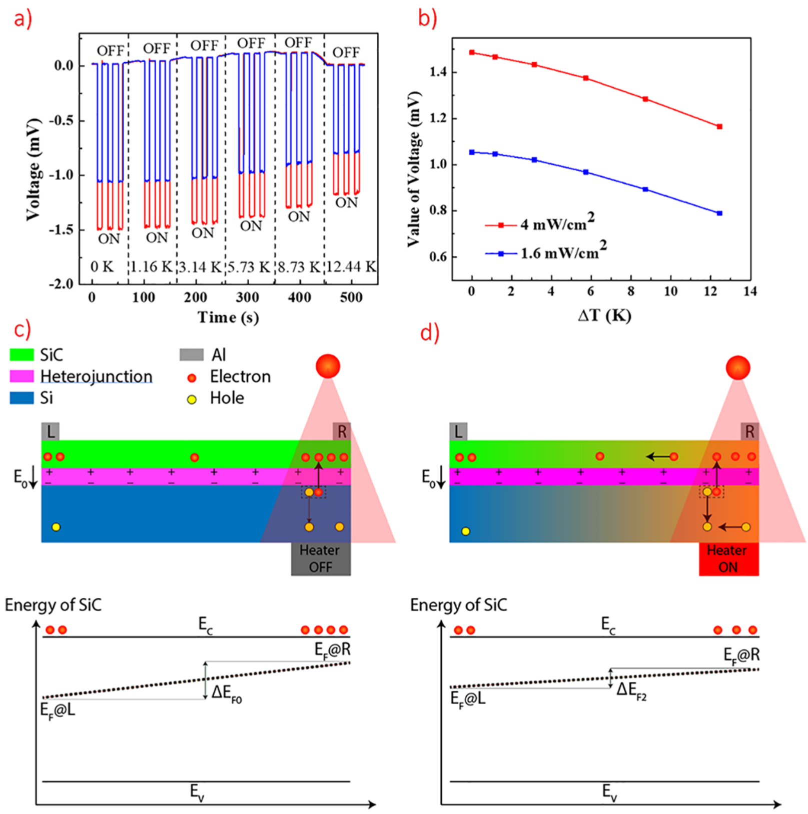

Figure 4. Desensitization by compensating light gradient and temperature gradient: illuminating and heating the electrode R. (a) Real-time-generated voltage under illumination and temperature gradient. (b) Dependence of voltage by temperature differences between the two electrodes. (c) Process of photonic excitation leads to the generation of EHPs and the resultant uneven distribution of electrons in a 3C-SiC layer, as well as the alteration of the band structure of 3C-SiC under nonuniform light conditions. (d) Mechanism of generation of EHPs through a combination of photonic and thermal stimulation and the effect on the distribution of electrons and the energy band structure in 3C-SiC. The red lines represent 4 mW/cm^2 and the blue lines represent 1.6 mW/cm^2.

increases, the current value also increases, owing to the presence of additional free electrons in the conduction band of the SiC layer. Similarly, increasing the temperature gradient across the device results in an increase in recorded currents, and this trend holds true across various light intensities. When a temperature gradient is applied to a semiconductor material, it generates an electric field and enhances the photocurrent generated by the photovoltaic effect. Furthermore, since the temperature gradients were produced by nonuniformly heating the electrodes, the rise in temperature can excite the electrons, leading to an increase in the electron concentration in the *n*-SiC layer and contributing to an increase in photocurrent.

To validate our hypothesis on the tunability of the photovoltage under the impact of the direction of a thermal gradient, we performed an additional experiment that involved the application of a laser beam to the electrode R and a heater under the electrode R. The photovoltage was recorded while the light intensity was varied, and the temperature gradient was introduced. The data from the validation test are presented in Figure 4a,b. In the absence of light, the photovoltage was nearly zero. When illuminated with light intensities of 1.6 and 4 mW/cm^2, the photovoltage was measured to be −1.05 and −1.5 mV, respectively. The results were consistent and repeatable over three cycles of turning on and off the laser source. Upon the introduction of a temperature gradient by heating electrode R, the measured voltage started to decrease. The photovoltage value decreased from 1.05 to 0.79 mV when the temperature gradient rose from 0 to 12.44 K for the 1.6 mW/cm^2 light intensity. A similar trend was observed for the 4 mW/cm^2 light intensity, with the photovoltage values of 1.49 and 1.17 mV for the temperature gradients of 0 to 12.44 K, respectively. This decline in photovoltage was observed for both light intensities and can be explained by the combination of the photovoltaic effect and the Seebeck effect.

The band structure of SiC is illustrated in Figure 4c,d. When the laser beam illuminates the surrounding area of electrode R, the photons pass through the thin SiC layer that has a large band gap and are absorbed by the Si layer, creating EHPs. The built-in electric field pushes the electrons toward the SiC layer, creating a high concentration of electrons at electrode R. The voltage recorded when illuminating electrode R is negative compared to the voltage measured when illuminating electrode L.

When the heater under the electrode R was turned on and a temperature gradient was created across the sensor, the hot temperature diffused the electrons toward the electrode L. This diffusion resulted in a decrease in the electron concentration gradient compared to that when illuminating alone. The Fermi level at the electrode L was lowered while the Fermi level at the electrode R was lifted, and this shift in the Fermi levels had an impact on the generated voltage. The voltage generated by the temperature gradient counteracted the photovoltage, and as a result, the measured voltage when applying illumination and a hot temperature at the same electrode was found to be lower than that when applying illumination alone. Furthermore, when the temperature gradient between the two

https://doi.org/10.1021/acsami.3c06699
ACS Appl. Mater. Interfaces 2023, 15, 38930−38937

electrodes increased, the generated voltage decreased. When increasing ΔT between the two electrodes to 12.44 K by heating the electrode R to 440 K, the high temperature excites the electrons from the valence band to the conduction band of Si and also enhances the electrical conductivity of the SiC layer. The elevated temperature induced an increase in the number of free electrons in the Si layer, and these electrons are subsequently driven toward SiC, which results in a decrease in the electron gradient between the two electrodes and a decrease in the recorded voltage.

■ CONCLUSIONS

In conclusion, this study has successfully demonstrated the use of lateral temperature gradients in 3C-SiC/Si heterostructures for enhancing the photovoltaic effect. We successfully utilized a conventional photolithography and etching process to fabricate the heterostructure-based microsensors, with their photovoltaic behavior significantly improved by using the temperature gradient. The photovoltage was improved up to 51% when the temperature gradient between two electrodes is 8.73 K. These findings could be used in the development of ultrasensitive self-powered microsensors. Our study also provides valuable insights into the relationship between temperature gradients, Fermi levels, and the generated photovoltage in self-powered sensors. Temperature gradients can have a significant impact on the performance of these sensors and should be considered in the design and implementation of self-powered sensing systems. It is worth noting that this effect is not limited to the specific experiment we performed, but it could be observed in any scenario where the temperature gradient and light are applied to the same heterostructure. This can be a useful information for future research and development in the field of thermophotovoltaics. This study highlights the necessity for further research in this sector to optimize the use of temperature gradients and other energy sources for maximum energy efficiency and reliable performance.

■ EXPERIMENTAL SECTION

We have successfully fabricated a *n*-SiC/*p*-Si heterostructure-based device to examine the impact of temperature gradient on the photovoltaic effect. Starting from a commercially available *p*-type silicon wafer, a 100 nm SiC film was deposited using a low-pressure chemical vapor deposition (LPCVD) process in a hot chamber at a temperature of 1000 °C. The doping concentration of the *n*-SiC layer and *p*-Si layer is about 10^{19} and 5×10^{14} cm^{-3}, respectively (step 1). Following this, an Al layer was sputtered on the SiC/Si wafer by a metal-sputtering machine (step 2), and the wafer was then coated with a photoresist (step 3). A photolithography process was employed to etch Al and create the suitable shapes of electrodes (step 4), and another photolithography process and a photoresist were utilized to etch SiC to create the desired structures of the SiC layer (step 5). The wafer was finally diced to achieve the desired shape of the device for testing (step 6).

An atomic force microscope (model: MFP3D-BIO) was employed to measure the surface topography of the 3C-SiC film on Si. The efficacy of the growth can be determined by the root-mean-square of surface roughness. To see the structure of the sensors that were made utilizing the photolithography method, a SEM image was taken. After that, the sensor was examined to determine whether the sensor has Ohmic contact and is suitable for electrical characterization.

The device was mounted on a hot plate of the Linkam HFS600E-PB4 device to establish a temperature gradient across the device, as shown in Figure S1. The Linkam HFS600E-PB4 device could precisely regulate the temperature within 0.1°C. During the experiment, a red laser beam with a wavelength of 635 nm was applied to the top of the sensor. The interplay of light illumination and temperature gradient could be studied by adjusting the position of the focused laser beam to illuminate either electrode R in the heated region or electrode L in the unheated region. Figure S2a demonstrates the application of a hot plate to heat the electrode R and a laser beam to illuminate the electrode L. Figure S2b illustrates the simultaneous application of both the laser beam and hot temperature to the electrode R. The open-circuit voltage between the two electrodes was measured when changing the illuminating condition, illuminating position, and the value of temperature gradient.

■ ASSOCIATED CONTENT

Supporting Information

The Supporting Information is available free of charge at https://pubs.acs.org/doi/10.1021/acsami.3c06699.

> Temperature gradient with the respective temperature at electrodes; comparative data of recent works; picture of the device; and schematic view of the experiment (PDF)

■ AUTHOR INFORMATION

Corresponding Authors

Hung Nguyen − *School of Engineering and Centre for Future Materials, University of Southern Queensland, Toowoomba, Queensland 4350, Australia*; orcid.org/0000-0001-9887-3691; Email: hung.nguyen@usq.edu.au

Toan Dinh − *School of Engineering and Centre for Future Materials, University of Southern Queensland, Toowoomba, Queensland 4350, Australia*; Email: toan.dinh@usq.edu.au

Authors

Thanh Nguyen − *School of Engineering and Centre for Future Materials, University of Southern Queensland, Toowoomba, Queensland 4350, Australia*; orcid.org/0000-0002-3213-6178

Duy Van Nguyen − *School of Engineering and Centre for Future Materials, University of Southern Queensland, Toowoomba, Queensland 4350, Australia*

Hoang-Phuong Phan − *School of Mechanical and Manufacturing Engineering, University of New South Wales, Sydney, New South Wales 2052, Australia*; orcid.org/0000-0002-1724-5667

Tuan Khoa Nguyen − *Queensland Micro- and Nanotechnology Centre, Griffith University, Nathan, Queensland 4111, Australia*; orcid.org/0000-0003-1271-9576

Dzung Viet Dao − *Queensland Micro- and Nanotechnology Centre, Griffith University, Nathan, Queensland 4111, Australia*; orcid.org/0000-0002-6348-0879

Nam-Trung Nguyen − *Queensland Micro- and Nanotechnology Centre, Griffith University, Nathan, Queensland 4111, Australia*

John Bell − *School of Engineering, University of Southern Queensland, Toowoomba, Queensland 4350, Australia*

Complete contact information is available at: https://pubs.acs.org/10.1021/acsami.3c06699

Notes

The authors declare no competing financial interest.

https://doi.org/10.1021/acsami.3c06699
ACS Appl. Mater. Interfaces 2023, 15, 38930−38937

ACKNOWLEDGMENTS

The research was funded by the Australian Research Council through grants DE210100852 and DP220101252. The 3C-SiC/Si material was provided by the Queensland Microtechnology Facility, a part of the Griffith Queensland node of the Australian National Fabrication Facility, a company created under the National Collaborative Research Infrastructure Strategy to offer nano and microfabrication services for Australian researchers.

REFERENCES

(1) Gao, T.; Ji, Y.; Yang, Y. Thermo-Phototronic-Effect-Enhanced Photodetectors Based on Porous ZnO Materials. *Adv. Electron. Mater.* **2019**, *5*, No. 1900776.
(2) Le, X.; Shi, Q.; Vachon, P.; Ng, E. J.; Lee, C. Piezoelectric MEMS—Evolution from Sensing Technology to Diversified Applications in the 5G/Internet of Things (IoT) Era. *J. Micromech. Microeng.* **2021**, *32*, No. 014005.
(3) Ilderem, V. The Technology Underpinning 5G. *Nat. Electron.* **2020**, *3*, 5−6.
(4) Ashleibta, A. M.; Taha, A.; Khan, M. A.; Taylor, W.; Tahir, A.; Zoha, A.; Abbasi, Q. H.; Imran, M. A. 5g-Enabled Contactless Multi-User Presence and Activity Detection for Independent Assisted Living. *Sci. Rep.* **2021**, *11*, 17590.
(5) Dutta, T.; Kim, K.-H.; Deep, A.; Szulejko, J. E.; Vellingiri, K.; Kumar, S.; Kwon, E. E.; Yun, S.-T. Recovery of Nanomaterials from Battery and Electronic Wastes: A New Paradigm of Environmental Waste Management. *Renewable Sustainable Energy Rev.* **2018**, *82*, 3694−3704.
(6) Yao, L. P.; Zeng, Q.; Qi, T.; Li, J. An Environmentally Friendly Discharge Technology to Pretreat Spent Lithium-Ion Batteries. *J. Cleaner Prod.* **2020**, *245*, No. 118820.
(7) Park, S.; Jeong, S. Y.; Lee, T. K.; Park, M. W.; Lim, H. Y.; Sung, J.; Cho, J.; Kwak, S. K.; Hong, S. Y.; Choi, N.-S. Replacing Conventional Battery Electrolyte Additives with Dioxolone Derivatives for High-Energy-Density Lithium-Ion Batteries. *Nat. Commun.* **2021**, *12*, 838.
(8) Larcher, D.; Tarascon, J.-M. Towards Greener and More Sustainable Batteries for Electrical Energy Storage. *Nat. Chem.* **2015**, *7*, 19−29.
(9) Nguyen, T.; Van Nguyen, D.; Nguyen, H.; Tong, B.; Tran, C.-D.; Takahashi, H.; Nguyen, N.-T.; Dao, D. V.; Dinh, T. Light Harvesting Self-Powered Strain Sensor using 3C-SiC/Si Heterostructure. *IEEE Sens.* **2022**, 1−4.
(10) Hao, S.; Jiao, J.; Chen, Y.; Wang, Z. L.; Cao, X. Natural Wood-Based Triboelectric Nanogenerator as Self-Powered Sensing for Smart Homes and Floors. *Nano Energy* **2020**, *75*, No. 104957.
(11) Meng, J.; Li, Q.; Huang, J.; Pan, C.; Li, Z. Self-Powered Photodetector for Ultralow Power Density UV Sensing. *Nano Today* **2022**, *43*, No. 101399.
(12) Nguyen, T.; Dinh, T.; Nguyen, H.; Vu, T. H.; Tran, C.-D.; Song, P.; Bell, J.; Nguyen, N.-T.; Dao, D. V. The Concept of Light-Harvesting, Self-Powered Mechanical Sensors Using a Monolithic Structure. *Nano Energy* **2022**, *96*, No. 107030.
(13) Tan, Y. K.; Panda, S. K. Energy Harvesting from Hybrid Indoor Ambient Light and Thermal Energy Sources for Enhanced Performance of Wireless Sensor Nodes. *IEEE Trans. Ind. Electron.* **2011**, *58*, 4424−4435.
(14) Li, Q.; Huang, J.; Meng, J.; Li, Z. Enhanced Performance of a Self-Powered ZnO Photodetector by Coupling LSPR-Inspired Pyro-Phototronic Effect and Piezo-Phototronic Effect. *Adv. Opt. Mater.* **2022**, *10*, No. 2102468.
(15) Li, Q.; Meng, J.; Huang, J.; Li, Z. Plasmon-Induced Pyro-Phototronic Effect Enhancement in Self-Powered UV−Vis Detection with a ZnO/CuO p−n Junction Device. *Adv. Funct. Mater.* **2022**, *32*, No. 2108903.
(16) Cuadras, A.; Gasulla, M.; Ferrari, V. Thermal Energy Harvesting Through Pyroelectricity. *Sens. Actuators, A* **2010**, *158*, 132−139.
(17) Carvalho, C.; Paulino, N. On the Feasibility of Indoor Light Energy Harvesting for Wireless Sensor Networks. *Procedia Technol.* **2014**, *17*, 343−350.
(18) Saraf, R.; Pu, L.; Maheshwari, V. A Light Harvesting, Self-Powered Monolith Tactile Sensor Based on Electric Field Induced Effects in MAPbI3 Perovskite. *Adv. Mater.* **2018**, *30*, No. 1705778.
(19) Jimenez-Jorquera, C.; Orozco, J.; Baldi, A. ISFET Based Microsensors for Environmental Monitoring. *Sensors* **2010**, *10*, 61−83.
(20) Rogers, C.; Piggott, A. Y.; Thomson, D. J.; Wiser, R. F.; Opris, I. E.; Fortune, S. A.; Compston, A. J.; Gondarenko, A.; Meng, F.; Chen, X.; Reed, G. T.; Nicolaescu, R. A Universal 3D Imaging Sensor on a Silicon Photonics Platform. *Nature* **2021**, *590*, 256−261.
(21) Mennel, L.; Symonowicz, J.; Wachter, S.; Polyushkin, D. K.; Molina-Mendoza, A. J.; Mueller, T. Ultrafast Machine Vision with 2D Material Neural Network Image Sensors. *Nature* **2020**, *579*, 62−66.
(22) Vicente, A. T.; Araújo, A.; Mendes, M. J.; Nunes, D.; Oliveira, M. J.; Sanchez-Sobrado, O.; Ferreira, M. P.; Águas, H.; Fortunato, E.; Martins, R. Multifunctional Cellulose-Paper for Light Harvesting and Smart Sensing Applications. *J. Mater. Chem. C* **2018**, *6*, 3143−3181.
(23) Foisal, A. R. M.; Dinh, T.; Nguyen, V. T.; Tanner, P.; Phan, H.-P.; Nguyen, T.-K.; Haylock, B.; Streed, E. W.; Lobino, M.; Dao, D. V. Self-Powered Broadband (UV-NIR) Photodetector Dased on 3C-SiC/Si Heterojunction. *IEEE Trans. Electron Devices* **2019**, *66*, 1804−1809.
(24) Du, X.; Tian, W.; Pan, J.; Hui, B.; Sun, J.; Zhang, K.; Xia, Y. Piezo-Phototronic Effect Promoted Carrier Separation in Coaxial p-n Junctions For Self-Powered Photodetector. *Nano Energy* **2022**, *92*, No. 106694.
(25) Zhang, K.; Yang, Y. Thermo-Phototronic Effect Enhanced InP/ZnO Nanorod Heterojunction Solar Cells for Self-Powered Wearable Electronics. *Adv. Funct. Mater.* **2017**, *27*, No. 1703331.
(26) Yang, L.; Wu, L.; Su, L.; Xu, L.; Zhao, L.-D.; Yang, Y. Enhanced Photodetector at Low-Temperature via Thermo-Phototronic Effect in N-type SnSe: Br Single Crystal. *Nano Energy* **2023**, *107*, No. 108140.
(27) Lv, B.; Liu, Y.; Wu, W.; Xie, Y.; Zhu, J.-L.; Cao, Y.; Ma, W.; Yang, N.; Chu, W.; Jia, Y.; Wei, J.; Sun, J. L. Local Large Temperature Difference and Ultra-Wideband Photothermoelectric Response of The Silver Nanostructure Film/Carbon Nanotube Film Heterostructure. *Nat. Commun.* **2022**, *13*, 1835.
(28) Nguyen, H.; Nguyen, T.; Van Nguyen, D.; Phan, H.-P.; Nguyen, N.-T.; Dao, D.; Bell, J.; Dinh, T. Thermo-Phototronic Effect for Self-Powered Photodetector Using n-3C-SiC/p-Si Heterostructure. In *IEEE Sensors*, 2022, IEEE; pp 1−4. https://ieeexplore.ieee.org/abstract/document/9967105.
(29) Ouyang, B.; He, W.; Wu, L.; Zhao, L.-D.; Yang, Y. Thermo-Phototronic Effect in p-type Na-Doped SnS Single Crystals for Enhanced Self-Powered Photodetectors. *Nano Energy* **2021**, *88*, No. 106268.
(30) Dinh, T.; Nguyen, T.; Foisal, A.; Phan, H.-P.; Nguyen, T.-K.; Nguyen, N.-T.; Dao, D. Optothermotronic Effect as an Ultrasensitive Thermal Sensing Technology for Solid-State Electronics. *Sci. Adv.* **2020**, *6*, 2671.
(31) Foisal, A. R. M.; Nguyen, T.; Dinh, T.; Nguyen, T. K.; Tanner, P.; Streed, E. W.; Dao, D. V. 3C-SiC/Si Heterostructure: An Excellent Platform for Position-Sensitive Detectors Based on Photovoltaic Effect. *ACS Appl. Mater. Interfaces* **2019**, *11*, 40980−40987.
(32) Andersson, M.; Pearce, R.; Spetz, A. L. New Generation SiC Based Field Effect Transistor Gas Sensors. *Sens. Actuators, B* **2013**, *179*, 95−106.
(33) Phan, H.-P. Introduction and Literature Review. In *Piezoresistive Effect of p-Type Single Crystalline 3C-SiC: Silicon Carbide Mechanical Sensors for Harsh Environments*; Springer International Publishing, 2017; pp 1−30. https://link.springer.com/chapter/10.1007/978-3-319-55544-7_1.

(34) Nguyen, T. K.; Aberoumand, S.; Dao, D. V. Advances in Si and SiC Materials for High-Performance Supercapacitors toward Integrated Energy Storage Systems. *Small* **2021**, *17*, No. 2101775.
(35) Zhang, X.; Liu, B.; Yang, W.; Jia, W.; Li, J.; Jiang, C.; Jiang, X. 3D-Branched Hierarchical 3C-SiC/ZnO Heterostructures for High-Performance Photodetectors. *Nanoscale* **2016**, *8*, 17573−17580.
(36) Mailoa, J. P.; Akey, A. J.; Simmons, C. B.; Hutchinson, D.; Mathews, J.; Sullivan, J. T.; Recht, D.; Winkler, M. T.; Williams, J. S.; Warrender, J. M.; Persans, P. D.; Aziz, M. J.; Buonassisi, T. Room-Temperature Sub-Band Gap Optoelectronic Response of Hyperdoped Silicon. *Nat. Commun.* **2014**, *5*, 3011.
(37) Kasap, S. *Principles of Electronic Materials and Devices*; 4th ed., 2018; pp 411−526.
(38) Qi, J.; Ma, N.; Ma, X.; Adelung, R.; Yang, Y. Enhanced Photocurrent in BiFeO3 Materials by Coupling Temperature and Thermo-Phototronic Effects for Self-Powered Ultraviolet Photodetector System. *ACS Appl. Mater. Interfaces* **2018**, *10*, 13712−13719.
(39) Ouyang, B.; Zhang, K.; Yang, Y. Self-Powered UV Photodetector Array Based on P3HT/ZnO Nanowire Array Heterojunction. *Adv. Mater. Technol.* **2017**, *2*, No. 1700208.

https://doi.org/10.1021/acsami.3c06699
ACS Appl. Mater. Interfaces 2023, 15, 38930−38937